Supporting information

Quantitative analysis of intermolecular interactions in cocrystals and a pair of polymorphous cocrystal hydrates from 1,4-dihydroquinoxaline-2,3-dione and 1*H*-benzo[*d*]imidazol-2(3*H*)-one with 2,5-dihydroxy-1,4-benzoquinones: A combined X-ray structure and theoretical analysis

Martha V. Sosa-Rivadeneyra,[a]* Perumal Venkatesan,[b] Fermin Flores-Manuel,[a] Sylvain Bernès,[c] Herbert Höpfl,[d] Margarita Cerón,[b] Subbiah Thamotharan[e] and M. Judith Percino[b]

[a]Facultad de Ciencias Químicas, Benemérita Universidad Autónoma de Puebla (BUAP). 14 Sur Esquina San Claudio, San Manuel, 72570, Puebla, Mexico

[b]Unidad de Polímeros y Electrónica Orgánica, Instituto de Ciencias, Benemérita Universidad Autónoma de Puebla, Val3-Ecocampus Valsequillo, Independencia O2 Sur 50, San Pedro Zacachimalpa, C.P. 72960 Puebla, Mexico

[c]Instituto de Física, Benemérita Universidad Autónoma de Puebla (IFBUAP). Av. San Claudio y Blvd. 18 Sur, Col. San Manuel 72570, Puebla, Mexico

[d]Centro de Investigaciones Químicas, Instituto de Investigación en Ciencias Básicas y Aplicadas, Universidad Autónoma del Estado de Morelos, Av. Universidad 1001, Cuernavaca 62209, Morelos, Mexico.

[e]Biomolecular Crystallography Laboratory, Department of Bioinformatics, School of Chemical and Biotechnology, SASTRA Deemed University, 613 401, Thanjavur, India.

Experimental procedures for the crystallization of compounds I, $I_A \cdot 2H_2O$, $I_B \cdot 2H_2O$, II and III

Screening experiments for cocrystal phases between the cyclic amides (DHQ or BIM) and the anilic acids (CA or AA) explored herein were realized using the slow solvent evaporation method. Initially, crystallization attempts were performed using a 1:1 stoichiometric ratio and the following solvents: acetone, MeOH, EtOH, CH_3CN and H_2O. However, in all cases where crystals suitable for single-crystal X-ray diffraction analysis were isolated, the amide-anilic acid proportion in the cocrystal was 2:1. Because of this, the crystallization experiments were then repeated using this ratio.

$(DHQ)_2CA$ (**I**): 1,4-Dihydroquinoxaline-2,3-dione (0.018 g, 0.111 mmol) and 2,5-dichloro-3,6-dihydroxy-*p*-benzoquinone (0.012 g, 0.055 mmol) were dissolved in 20 mL of acetonitrile. This mixture was heated until dissolution of the reactants, whereupon the solution was filtered and left for slow solvent evaporation at room temperature. After 3 days yellow crystals had formed, which were suitable for single-crystal X-ray diffraction analysis. Yield: 37%. IR (ATR): $\tilde{\upsilon}$ = 3031, 2954, 2868, 1666, 1626, 1402, 1362, 1254, 984, 845, 752, 701, 645, 566, 468 cm^{-1}.

$(DHQ)_2CA$ (**$I_A \cdot 2H_2O$**): 1,4-Dihydroquinoxaline-2,3-dione (0.018 g, 0.111 mmol) and 2,5-dichloro-3,6-dihydroxy-*p*-benzoquinone (0.012 g, 0.055mmol) were dissolved in 20 mL water and the mixture was heated until complete dissolution of the reactants. After filtration, the solution was left for slow solvent evaporation at room temperature. After 10 days red crystals had formed, which were suitable for single-crystal X-ray diffraction analysis. Yield: 55%. IR (ATR): $\tilde{\upsilon}$ = 3415, 3223, 3049, 2972, 2875, 1689, 1659, 1600, 1507, 1404, 1385, 1246, 1219, 1126, 1004, 938, 847, 797, 771, 746, 701, 667, 640, 582, 562, 467 cm^{-1}.

$(DHQ)_2CA$ (**$I_B \cdot 2H_2O$**): 1,4-Dihydroquinoxaline-2,3-dione (0.018 g, 0.111 mmol) and 2,5-dichloro-3,6-dihydroxy-*p*-benzoquinone (0.012 g, 0.055 mmol) were dissolved in 20 mL of methanol (hydrated) and the resultant mixture was heated until complete dissolution of the reactants. After filtration, the solution was left for slow solvent evaporation at room

temperature. After 4 days reddish orange crystals had grown, which were suitable for single-crystal X-ray diffraction analysis. This product crystallized as a mixture of **$I_A \cdot 2H_2O$** and **$I_B \cdot 2H_2O$,** and only were recognized until their characterization by single-crystal X-ray diffraction.

$(BIM)_2CA$ (**II**): 1*H*-benzo[*d*]imidazol-2(3*H*)-one (0.018 g, 0.134 mmol) and 2,5-dichloro-3,6-dihydroxy-*p*-benzoquinone (0.014 g, 0.067 mmol) were dissolved in 20 mL of acetonitrile. The solution was heated until complete dissolution of the reactants and, after filtration, left for slow solvent evaporation at room temperature. After 5 days orange crystals had grown, which were suitable for single-crystal X-ray diffraction analysis. Yield: 55%. IR (ATR): $\tilde{u}$ = 3230, 3023, 2901, 2809, 1736, 1666, 1631, 1483, 1360, 1268, 1197, 1026, 982, 855, 735, 702, 598, 571, 501 cm^{-1}.

$(BIM)_2AA$ (**III**): 1*H*-benzo[*d*]imidazol-2(3*H*)-one (0.020 g, 0.149 mmol) and 2,5-dihydroxy-1,4-benzoquinone (0.010 g, 0.0745 mmol) were dissolved in 20 mL of acetonitrile. The reaction mixture was heated until complete dissolution of the reactants and, after filtration left for slow solvent evaporation at room temperature. After 5 days orange crystals had grown, which were suitable for single-crystal X-ray diffraction analysis. Yield: 57%. IR (ATR): $\tilde{u}$ = 3138, 3027, 2901, 2801, 1704, 1651, 1622, 1481, 1381, 1305, 1270, 1208, 1027, 871, 824, 759, 734, 701, 667, 596, 501 cm^{-1}.

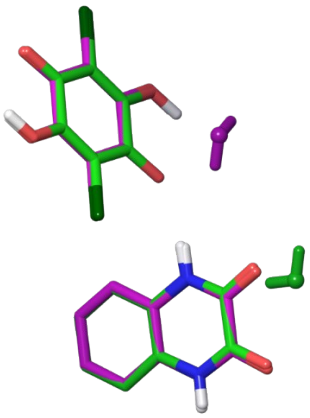

Figure S1. Structure overlay of the molecular components in **I**, **$I_A \cdot 2H_2O$** and **$I_B \cdot 2H_2O$**. For the structure overlay**,** atoms N1, C1, N2, C2, C9, C10, C9_a, C10_a were used. Color codes: C atoms and water molecule are green for **$I_A \cdot 2H_2O$** and purple for **$I_B \cdot 2H_2O$**.

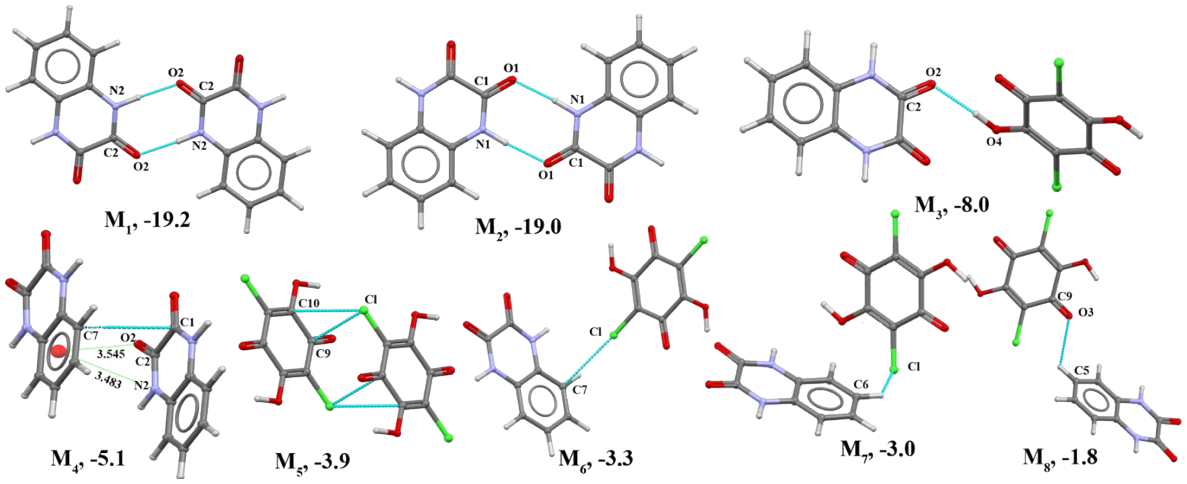

Figure S2. Homo- and heterodimeric motifs formed through hydrogen bonding and π···π contacts in the crystal structure of **I**. Dashed lines indicate the intermolecular interactions and the dimers are labeled along with the interaction energy obtained by DFT calculations (E_{tot} in kcal mol $^{-1}$, refer Table 2 in main manuscript).

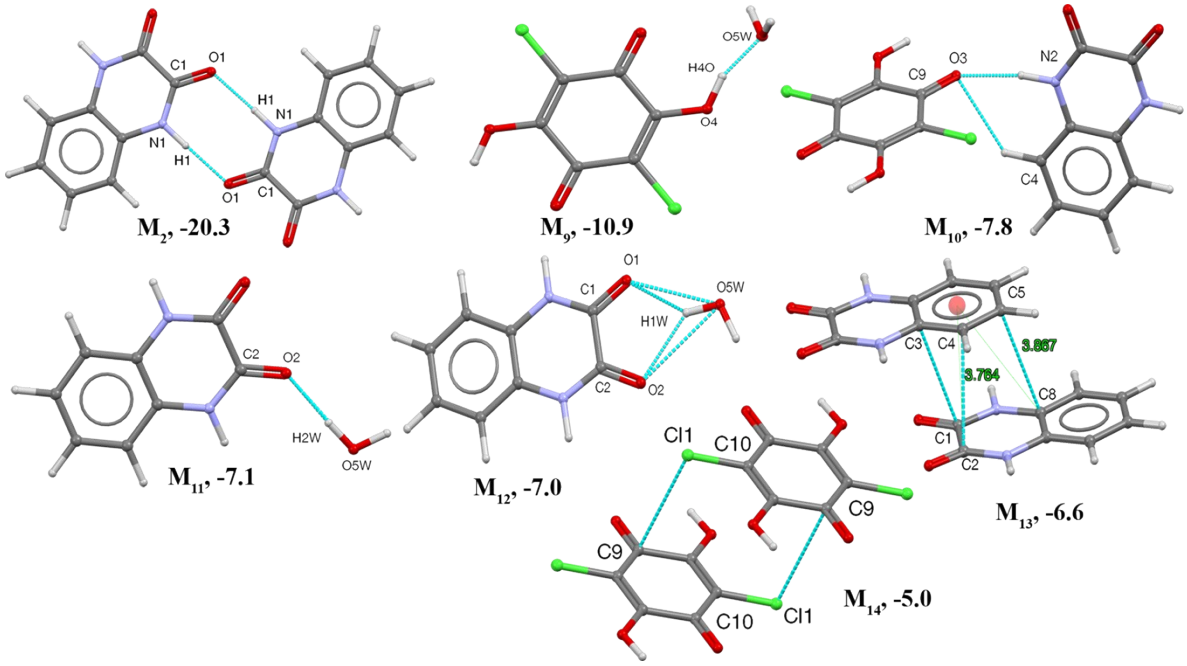

Figure S3. Homo- and heterodimeric motifs formed through hydrogen bonding and π···π contacts in the crystal structure of **I_A·2H_2O**. Dashed lines indicate the intermolecular interactions and the dimers are labeled along with the interaction energy obtained by DFT calculations (E_{tot} in kcal mol $^{-1}$, refer Table 2 in main manuscript).

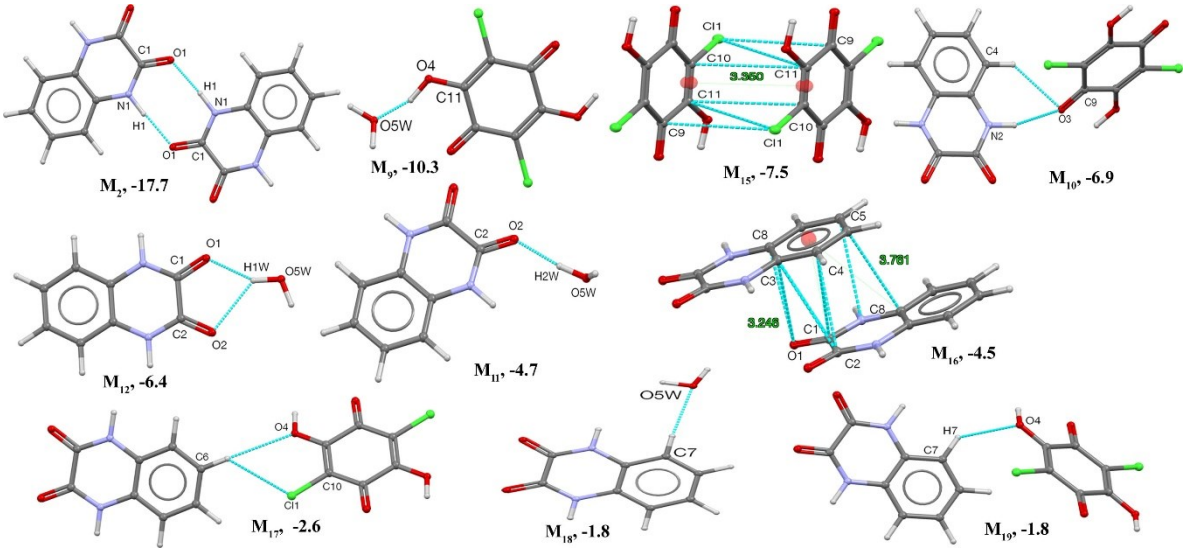

Figure S4. Homo- and heterodimeric motifs formed through hydrogen bonding and π···π contacts in the crystal structure of $\mathbf{I_B{\cdot}2H_2O}$. Dashed lines indicate the intermolecular interactions and the dimers are labeled along with the interaction energy obtained by DFT calculations (E_{tot} in kcal mol $^{-1}$, refer Table 2 in main manuscript).

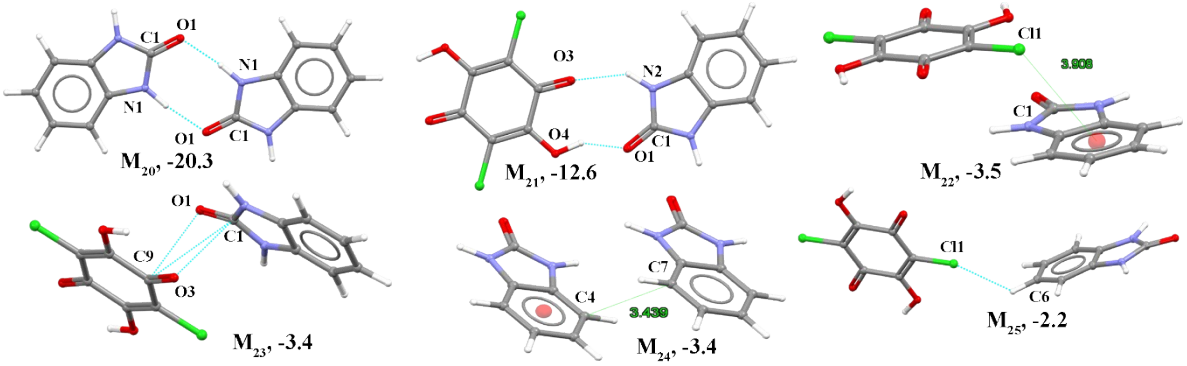

Figure S5. Homo- and heterodimeric motifs formed through hydrogen bonding and π···π contacts in the crystal structure of **II**. Dashed lines indicate the intermolecular interactions and the dimers are labeled along with the interaction energy obtained by DFT calculations (E_{tot} in kcal mol $^{-1}$, refer Table 2 in main manuscript).

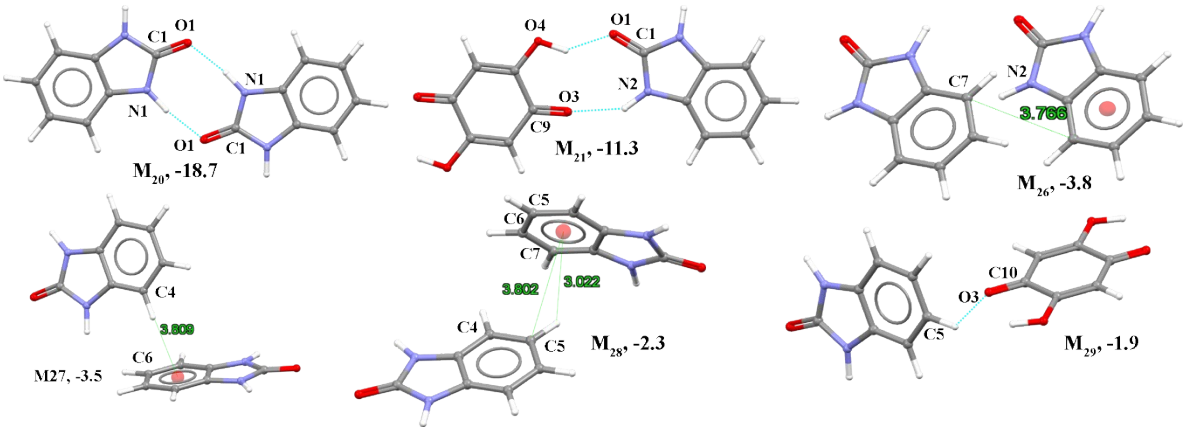

Figure S6. Homo- and heterodimeric motifs formed through hydrogen bonding and π···π contacts in the crystal structure of **III**. Dashed lines indicate the intermolecular interactions and the dimers are labeled along with the interaction energy obtained by DFT calculations (E_{tot} in kcal mol $^{-1}$, refer Table 2 in main manuscript).

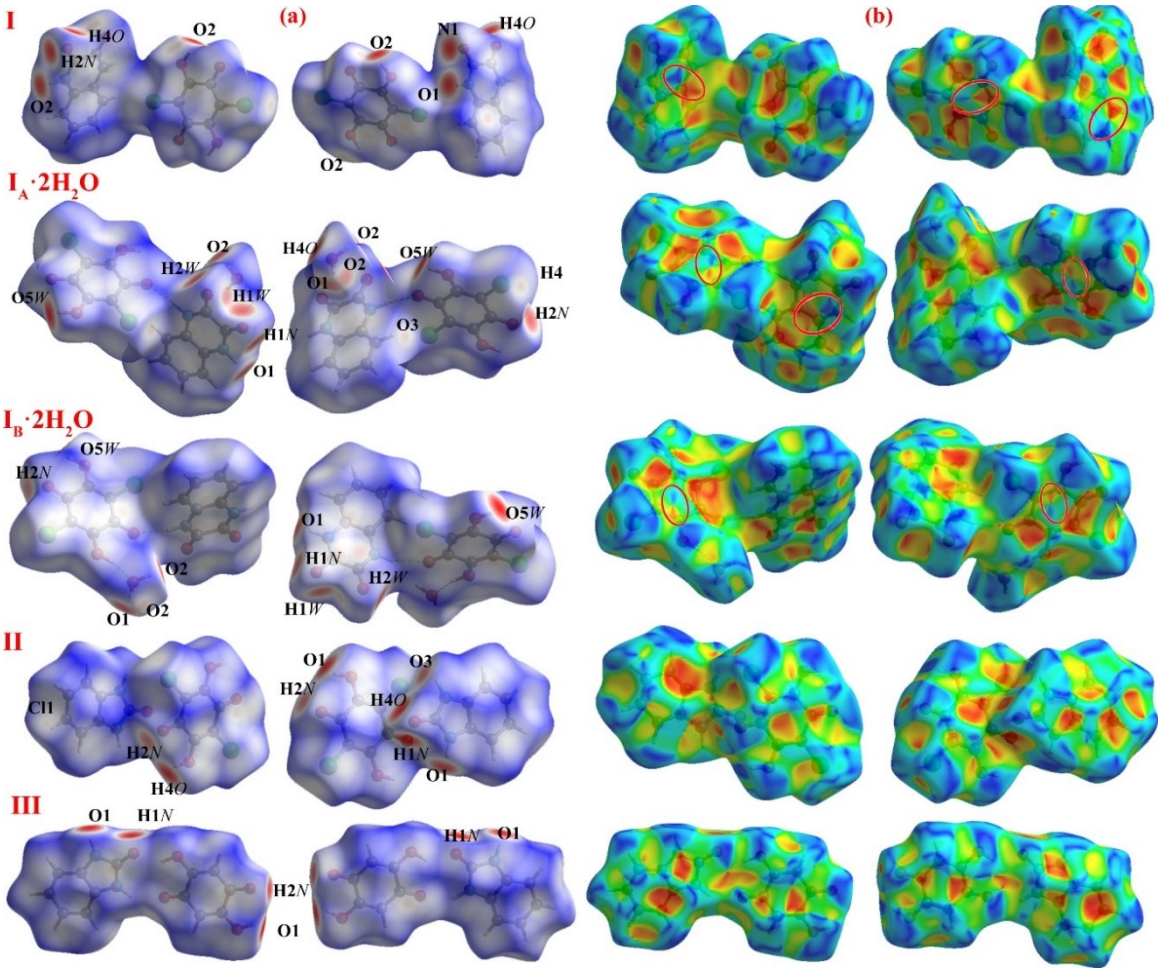

Figure S7. (a) Two different perspectives of the Hirshfeld surfaces mapped with d_{norm}. (b) Two different perspective views of the Hirshfeld shape index maps. Note: Red and blue triangles (circled) indicate the presence of π-stacking interactions in the respective compounds.

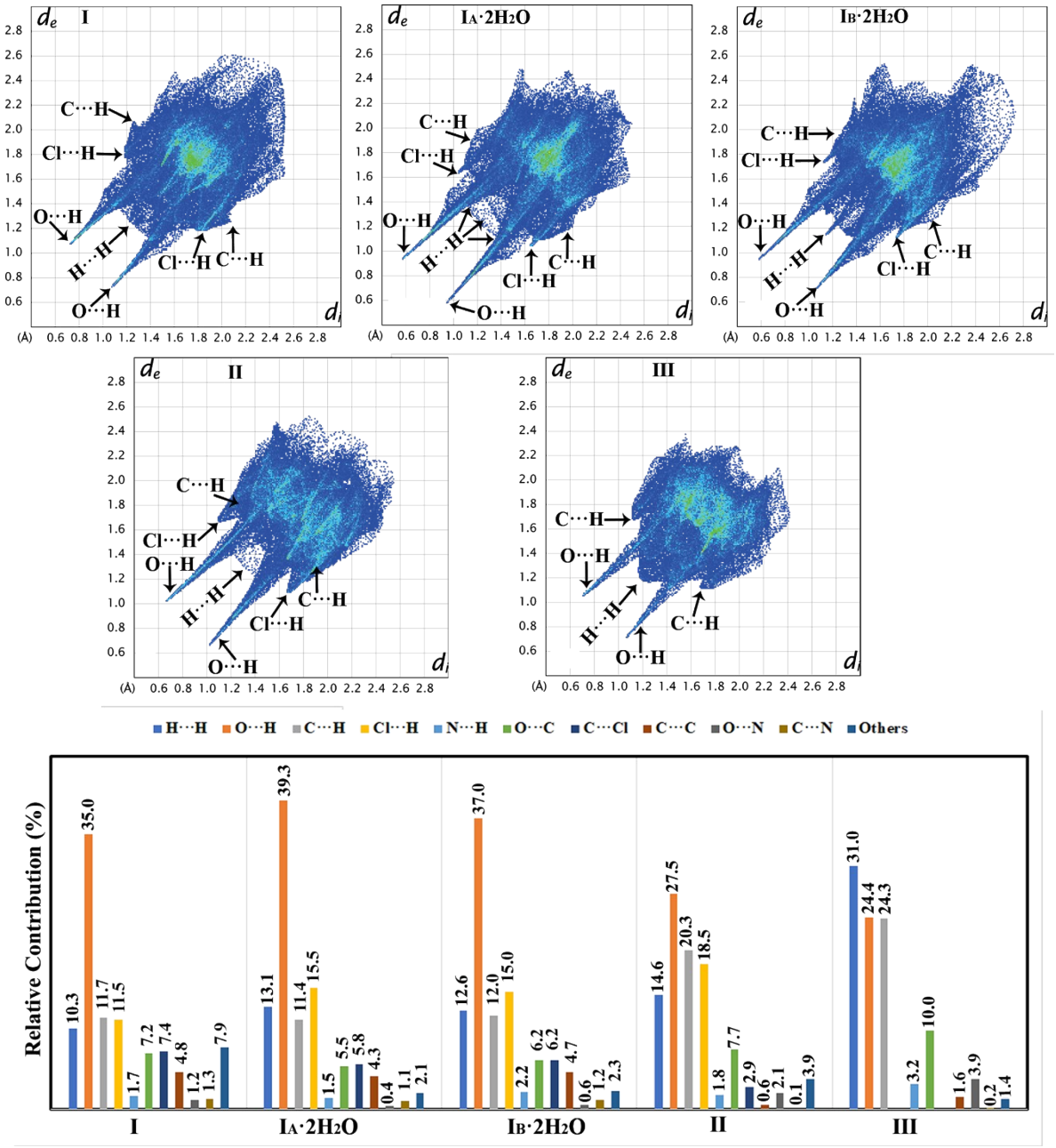

Figure S8. 2D Fingerprint (FP) plots for compounds **I**, **I_A·2H_2O**, **I_B·2H_2O**, **II** and **III** along with the relative contributions of the various intermolecular contacts in the crystal structures.

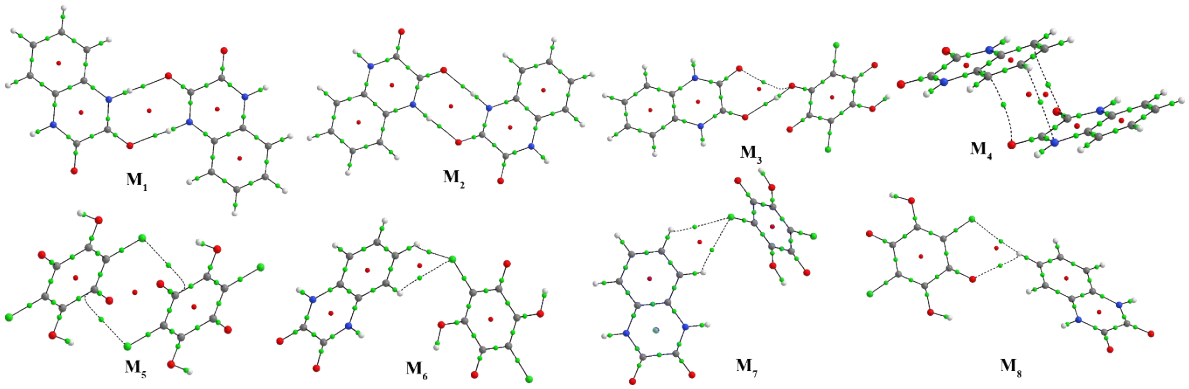

Figure S9. Molecular graphs with BCPs for selected molecular dimers in **I**. Small green spheres indicate the bond critical points (BCPs); and small red spheres indicate the ring critical points (RCPs).

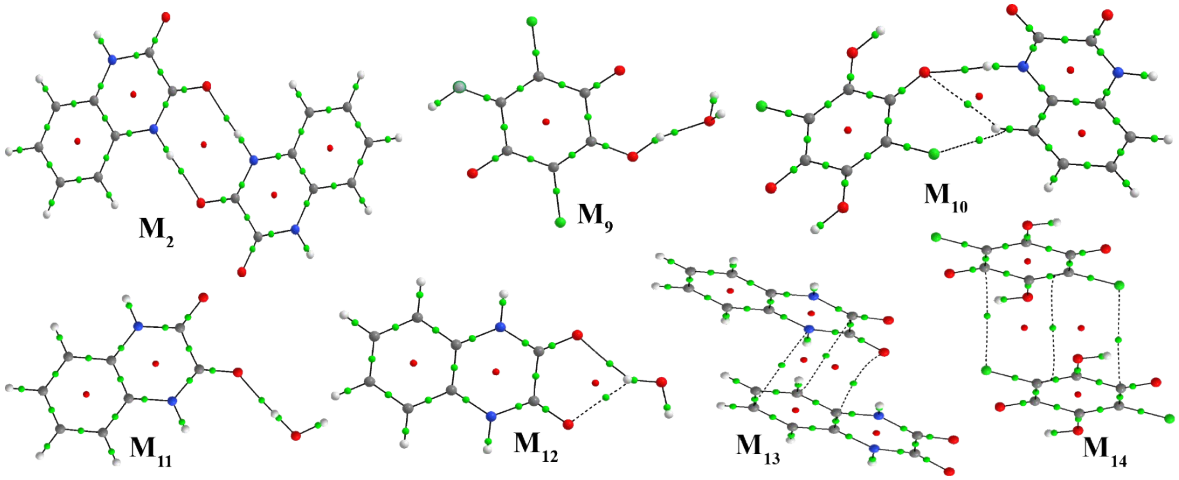

Figure S10. Molecular graphs with BCPs for selected molecular dimers in $\mathbf{I_A \cdot 2H_2O}$. Small green spheres indicate the bond critical points (BCPs); and small red spheres indicate the ring critical points (RCPs).

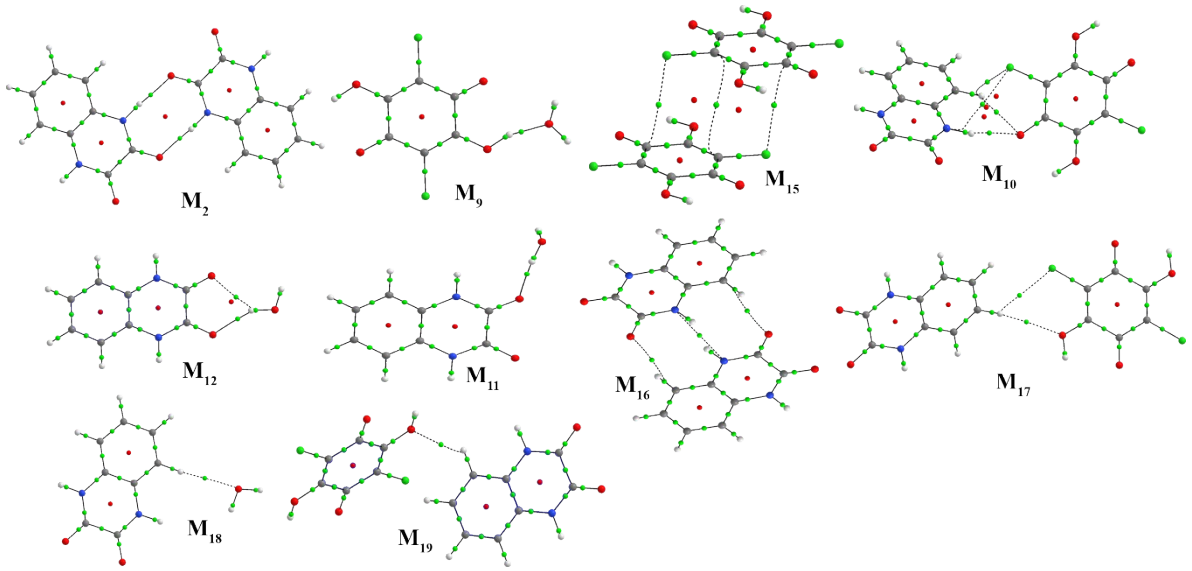

Figure S11. Molecular graphs with BCPs for selected molecular dimers in $\mathbf{I_B{\cdot}2H_2O}$. Small green spheres indicate the bond critical points (BCPs); and small red spheres indicate the ring critical points (RCPs).

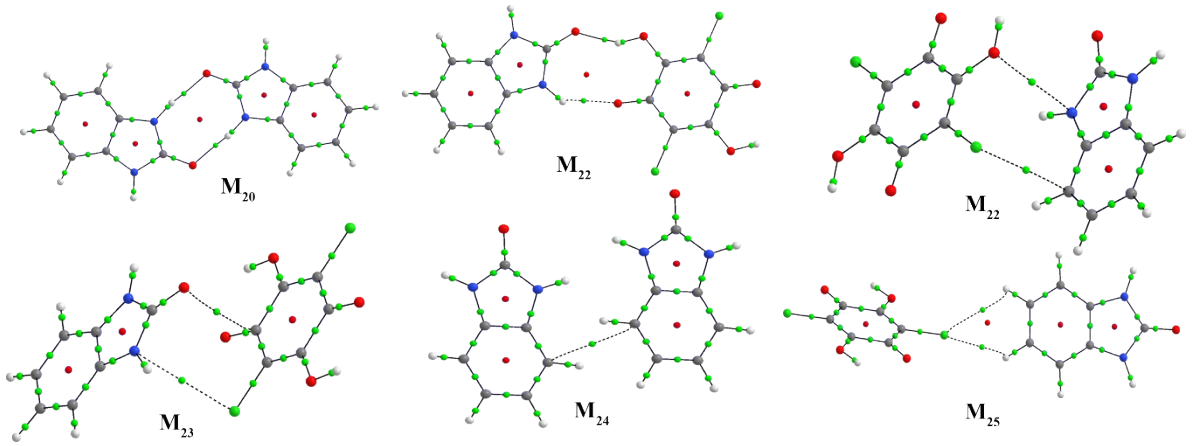

Figure S12. Molecular graphs with BCPs for selected molecular dimers in **II**. Small green spheres indicate the bond critical points (BCPs); and small red spheres indicate the ring critical points (RCPs).

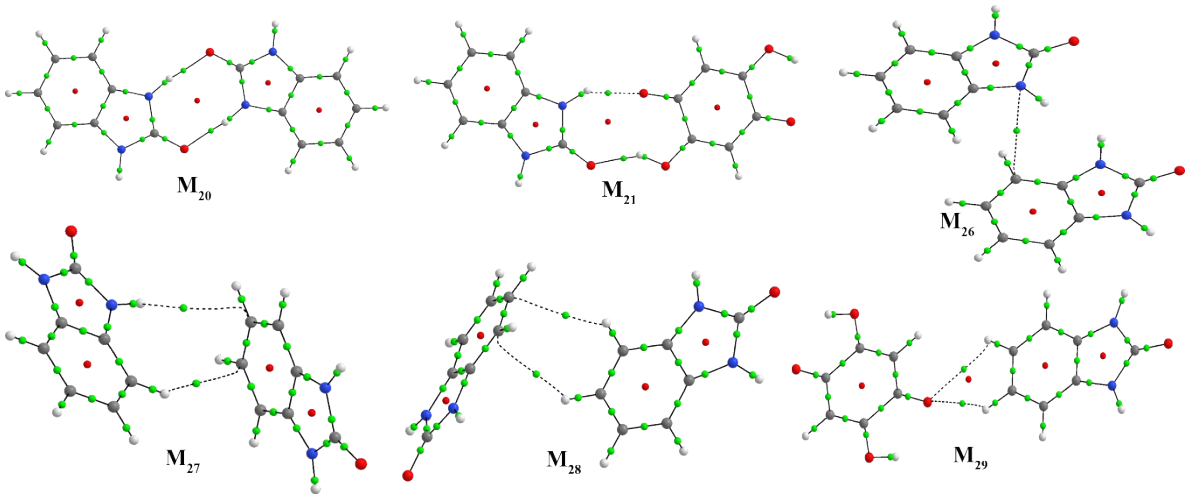

Figure S13. Molecular graphs with BCPs for selected molecular dimers in **III**. Small green spheres indicate the bond critical points (BCPs); and small red spheres indicate the ring critical points (RCPs).

Table S1. Crystallographic data and refinement parameters for compounds **I**, **I_A·2H_2O**, **I_B·2H_2O**, **II** and **III.**

	I	**I_A·2H_2O**	**I_B·2H_2O**	**II**	**III**
Deposition	CCDC-2016348	CCDC-2016349	CCDC-2016350	CCDC-2016351	CCDC-2016352
Formula	$C_6H_2Cl_2O_4$, $2(C_8H_6N_2O_2)$	$C_6H_2Cl_2O_4$, $2(C_8H_6N_2O_2)$, $2H_2O$	$C_6H_2Cl_2O_4$, $2(C_8H_6N_2O_2)$, $2H_2O$	$C_6H_2Cl_2O_4$, $2(C_7H_6N_2O)$	$C_6H_4O_4$, $2(C_7H_6N_2O)$
fw (g mol^{-1})	533.27	569.30	569.30	477.25	408.37
Shape/color	Plate/yellow	Irregular/red	Needle/orange	Prism/ orange	Block/orange
Space group	*P*-1	*P*-1	*C*2/*c*	$P2_1/n$	$P2_1/n$
Crystal size/mm^3	0.40 × 0.15 × 0.06	0.15 × 0.10 × 0.10	0.60 × 0.10 × 0.05	0.20 × 0.14 × 0.07	0.20 × 0.15 × 0.10
Diffractometer	Stoe-Stadivari	Stoe-Stadivari	Stoe-Stadivari	Stoe-Stadivari	Stoe-Stadivari
Temp. (K)	295(1)	295(1)	295(1)	295(1)	295(1)
Wavelength (Å)	0.56083	0.56083	0.56083	0.56083	0.56083
a (Å)	4.7921(5)	4.7183(6)	27.986(3)	8.4521(5)	5.2947(6)
b (Å)	11.1245(12)	10.9094(12)	4.6150(3)	5.1303(2)	8.1240(7)
c (Å)	11.2988(13)	11.9445(16)	24.046(2)	23.1482(14)	20.880(3)
α (°)	65.883(8)	74.120(9)	90	90	90
β (°)	86.445(9)	81.304(11)	132.364(5)	99.316(5)	90.109(9)
γ (°)	78.351(8)	81.681(10)	90	90	90
V (Å^3)	538.29(11)	581.11(13)	2294.7(4)	990.51(9)	898.13(17)
Z, Z'	1, 1/2	1, 1/2	4, 1/2	2, 1/2	2, 1/2
μ (mm^{-1})	0.194	0.187	0.189	0.201	0.070
ρ_{calcd} (Mg/m^{-3})	1.645	1.627	1.648	1.600	1.510
Transm. factors	0.654-1.000	0.497-1.000	0.325-1.000	0.492-1.000	0.352-1.000
Refl. collected	15290	13338	25780	20107	19443
Senθ/λ (Å^{-1})	0.68	0.64	0.64	0.64	0.64
R_{int}	0.042	0.069	0.109	0.045	0.070
Completeness	99.9%	99.9%	99.7%	99.6%	99.9
Data/param.	2879/172	2515/190	2487/187	2160/173	1966/146
Restraints	0	0	0	0	0
R_1, wR_2 [I>2σ(I)]	0.035, 0.085	0.034, 0.060	0.033, 0.058	0.036, 0.099	0.040, 0.094
R_1, wR_2 [all data]	0.055, 0.091	0.076, 0.068	0.068, 0.063	0.053, 0.104	0.057, 0.102
GOF on F^2	0.894	0.841	0.741	1.043	0.906

Table S2. Topological parameters from the QTAIM calculations for the intermolecular interactions observed in the molecular dimers of compound **I**. R_{ij}: Bond path, ρ: electron density (e/Å^3), $\nabla^2\rho$: Laplacian electron density (e/Å^5), V: potential energy density (a.u.); G: kinetic energy density (a.u.). $D.E._{(int)}$: dissociation energy = $-V \times 0.5$ (kcal mol^{-1}).

Dimer	Atoms[a]	R_{ij}	ρ	$\nabla^2\rho$	Ellipticity	V	G	$D.E._{(int)}$	$-V/G$
$\mathbf{M_1}$	H2N···O2	1.877	0.21498	2.40310	0.01573	-0.02856	0.02675	8.96	1.07
	O2···H2N	1.876	0.21503	2.40308	0.01572	-0.02857	0.02675	8.96	1.07
$\mathbf{M_2}$	O1···H1N	1.835	0.23872	2.54528	0.01411	-0.03311	0.02976	10.39	1.11
	H1N···O1	1.835	0.23872	2.54480	0.01410	-0.03310	0.02975	10.39	1.11
$\mathbf{M_3}$	H4O···O2	1.906	0.18362	2.23697	0.01678	-0.02365	0.02343	7.42	1.01
	O4···O1	3.056	0.06611	0.94886	1.23348	-0.00626	0.00805	1.96	0.78
$\mathbf{M_4}$	O2···C3	3.489	0.04161	0.50866	1.65211	-0.00309	0.00418	0.97	0.74
	C1···C7	3.353	0.04023	0.46919	0.28505	-0.00280	0.00384	0.88	0.73
	N2···C5	3.494	0.03718	0.42762	1.83371	-0.00250	0.00347	0.78	0.72
$\mathbf{M_5}$	C9···CL1	3.763	0.04696	0.60496	9.27398	-0.00351	0.00489	1.10	0.72
	CL1···C9	3.762	0.04695	0.60488	9.27232	-0.00351	0.00489	1.10	0.72
$\mathbf{M_6}$	CL1···H6	3.025	0.03909	0.46442	0.19368	-0.00278	0.00380	0.87	0.73
	CL1···H7	3.060	0.03636	0.43873	0.14273	-0.00260	0.00358	0.82	0.73
$\mathbf{M_7}$	CL1···H6	3.025	0.03910	0.46444	0.19370	-0.00281	0.00382	0.89	0.74
$\mathbf{M_8}$	CL1···H5	3.049	0.03300	0.39060	0.35331	-0.00226	0.00316	0.71	0.72
	O3···H5	2.549	0.05767	0.78046	0.18746	-0.00492	0.00651	1.54	0.76

[a] Atom numbering is as presented in Fig. 1.

Table S3. Topological parameters from the QTAIM calculations for the intermolecular interactions observed in the molecular dimers of compound **$I_A \cdot 2H_2O$**. R_{ij}: Bond path, ρ: electron density (e/Å^3), $\nabla^2\rho$: Laplacian electron density (e/Å^5), V: potential energy density (a.u.); G: kinetic energy density (a.u.). $D.E._{(int)}$: dissociation energy = $-V \times 0.5$ (kcal mol^{-1}).

Dimer	Atoms[a]	R_{ij}	ρ	$\nabla^2\rho$	Ellipticity	V	G	$D.E._{(int)}$	$-V/G$
M_2	H1N1···O1	1.869	0.22046	2.41088	0.01736	-0.02948	0.02725	9.25	1.08
	O1···H1N1	1.869	0.22046	2.41088	0.01736	-0.02948	0.02725	9.25	1.08
M_9	H4O···O5W	1.548	0.48001	2.80894	0.03222	-0.08565	0.05740	26.87	1.49
M_{10}	H2N2···O3	1.978	0.15564	2.18581	0.02224	-0.01917	0.02092	6.02	0.92
	H4···O3	2.687	0.04427	0.55242	0.25104	-0.00360	0.00467	1.13	0.77
	H4···CL1	3.654	0.02839	0.33573	0.57188	-0.00181	0.00265	0.57	0.68
M_{11}	O2···H2W	1.826	0.22414	2.58376	0.00463	-0.03211	0.02946	10.07	1.09
M_{12}	O1···H1W	2.000	0.15083	2.13581	0.06051	-0.01815	0.02015	5.69	0.90
	O2···H1W	2.236	0.09793	1.37033	0.27036	-0.00984	0.01203	3.09	0.82
M_{13}	C8···O1	3.742	0.04406	0.54411	2.39158	-0.00332	0.00448	1.04	0.74
	C4···C2	3.422	0.04126	0.48738	1.56088	-0.00288	0.00397	0.90	0.73
	C6···N1	3.495	0.04289	0.51495	2.63873	-0.00302	0.00418	0.95	0.72
M_{14}	C9···CL1	3.481	0.03785	0.47748	1.04276	-0.00272	0.00384	0.85	0.71
	C10···C10	4.415	0.03458	0.37901	8.87527	-0.00221	0.00307	0.69	0.72
	CL1···C9	3.481	0.03785	0.47745	1.04310	-0.00272	0.00384	0.85	0.71

[a] Atom numbering is as presented in Fig. 1.

Table S4. Topological parameters from the QTAIM calculations for the intermolecular interactions observed in the molecular dimers of compound **I_B·2H_2O**. R_{ij}: Bond path, ρ: electron density (e/Å^3), $\nabla^2\rho$: Laplacian electron density (e/Å^5), *V*: potential energy density (a.u.); *G*: kinetic energy density (a.u.). *D.E.*$_{(int)}$: dissociation energy = -*V* × 0.5 (kcal mol^{-1}).

Dimer	Atoms[a]	R_{ij}	ρ	$\nabla^2\rho$	Ellipticity	*V*	*G*	*D.E.*$_{(int)}$	-*V*/*G*
M_2	H1N1···O1	1.895	0.20577	2.34984	0.02131	-0.02680	0.02559	8.41	1.05
	O1···H1N1	1.895	0.20581	2.34989	0.02130	-0.02680	0.02559	8.41	1.05
M_9	H4O···O5W	1.558	0.46508	2.90048	0.03146	-0.08251	0.05630	25.89	1.47
M_{15}	CL1···C9	3.367	0.04792	0.61223	1.16083	-0.00373	0.00504	1.17	0.74
	C10···C10	4.083	0.04236	0.48442	8.64421	-0.00291	0.00397	0.91	0.73
	C9···CL1	3.367	0.04792	0.61226	1.15998	-0.00373	0.00504	1.17	0.74
M_{10}	H2N2···O3	2.116	0.11219	1.64387	0.01843	-0.01208	0.01457	3.79	0.83
	H4···O3	2.601	0.05087	0.64477	0.11656	-0.00420	0.00545	1.32	0.77
	H4···CL1	3.364	0.03824	0.45372	0.50046	-0.00264	0.00367	0.83	0.72
	H2···CL1	3.816	0.03510	0.43892	2.15223	-0.00262	0.00359	0.82	0.73
M_{12}	O1···H1W	1.927	0.17649	2.35416	0.02438	-0.02277	0.02359	7.14	0.96
	O2···H1W	2.446	0.06750	0.88538	1.00364	-0.00633	0.00776	1.99	0.82
M_{11}	O2···H2W	1.806	0.23982	2.61572	0.01325	-0.03493	0.03103	10.96	1.13
M_{16}	O1···C3	3.593	0.04916	0.61057	3.56585	-0.00386	0.00510	1.21	0.76
	C1···C4	3.718	0.04621	0.56438	44.75599	-0.00333	0.00459	1.04	0.73
	N1···C6	3.681	0.04668	0.58455	4.35668	-0.00343	0.00475	1.08	0.72
M_{17}	H6···CL1	3.024	0.03647	0.43745	0.03382	-0.00255	0.00354	0.80	0.72
	H6···O4	2.823	0.02854	0.36243	0.12462	-0.00230	0.00303	0.72	0.76
M_{18}	H7···O5W	2.739	0.03007	0.42017	0.08449	-0.00244	0.00340	0.76	0.72
M_{19}	H7···O4	2.696	0.05128	0.66923	0.44284	-0.00427	0.00561	1.34	0.76

[a] Atom numbering is as presented in Fig. 1.

Table S5. Topological parameters from the QTAIM calculations for the intermolecular interactions observed in the molecular dimers of compound **II**. R_{ij}: Bond path, ρ: electron density (e/Å^3), $\nabla^2\rho$: Laplacian electron density (e/Å^5), V: potential energy density (a.u.); G: kinetic energy density (a.u.). $D.E._{(int)}$: dissociation energy = $-V \times 0.5$ (kcal mol^{-1}).

Dimer	Atoms[a]	R_{ij}	ρ	$\nabla^2\rho$	Ellipticity	V	G	$D.E._{(int)}$	$-V/G$
M_{20}	O1···H1N	1.838	0.23397	2.52851	0.02736	-0.03208	0.02915	10.06	1.10
	H1N···O1	1.838	0.23391	2.52863	0.02737	-0.03207	0.02915	10.06	1.10
M_{21}	H4O···O1	1.707	0.30592	2.78951	0.00995	-0.04789	0.03842	15.03	1.25
	O3···H2N2	2.112	0.10682	1.78058	0.11685	-0.01149	0.01498	3.61	0.77
M_{22}	CL1···C7	3.465	0.04340	0.49256	0.10753	-0.00296	0.00404	0.93	0.73
M_{23}	C9···O1	3.178	0.04646	0.59457	0.96201	-0.00397	0.00507	1.25	0.78
	CL1···N2	3.454	0.04247	0.51871	0.51014	-0.00299	0.00419	0.94	0.71
M_{24}	C4···C7	3.459	0.03611	0.39747	3.29726	-0.00222	0.00317	0.70	0.70
M_{25}	CL1···H6	2.804	0.04985	0.69050	0.17776	-0.00411	0.00564	1.29	0.73
	CL1···H5	3.116	0.03470	0.46393	0.39510	-0.00259	0.00370	0.81	0.70

[a] Atom numbering is as presented in Fig. 1.

Table S6. Topological parameters from the QTAIM calculations for the intermolecular interactions observed in the molecular dimers of compound **III**. R_{ij}: Bond path, ρ: electron density (e/Å^3), $\nabla^2\rho$: Laplacian electron density (e/Å^5), V: potential energy density (a.u.); G: kinetic energy density (a.u.). $D.E._{(int)}$: dissociation energy = $-V \times 0.5$ (kcal mol^{-1}).

Dimer	Atoms[a]	R_{ij}	ρ	$\nabla^2\rho$	Ellipticity	V	G	$D.E._{(int)}$	$-V/G$
M_{20}	O1···H1N	1.821	0.24344	2.58256	0.02594	-0.03396	0.03038	10.65	1.12
	H1N···O1	1.821	0.24334	2.58282	0.02594	-0.03394	0.03037	10.65	1.12
M_{21}	H4O···O1	1.792	0.24802	2.75992	0.02884	-0.03595	0.03229	11.28	1.11
	O3···H2N2	2.016	0.13194	2.14183	0.09801	-0.01563	0.01893	4.91	0.83
M_{26}	C7···N2	3.532	0.03130	0.36104	0.71607	-0.00208	0.00291	0.65	0.71
M_{27}	H4···C6	2.888	0.04258	0.46919	1.20020	-0.00293	0.00390	0.92	0.75
	H2N2···C5	3.225	0.03014	0.36034	0.66945	-0.00211	0.00292	0.66	0.72
M_{28}	H4···C5	2.953	0.03724	0.42538	0.38102	-0.00252	0.00347	0.79	0.73
	H5···C4	3.074	0.03717	0.40718	1.20110	-0.00245	0.00334	0.77	0.73
M_{29}	H5···O3	2.587	0.05191	0.68662	0.11462	-0.00435	0.00574	1.36	0.76
	H6···O3	2.896	0.03412	0.43097	0.33912	-0.00282	0.00364	0.88	0.77

[a] Atom numbering is as presented in Fig. 1.